

Results of Lidar Studies of the Structure and Dynamics of Cirrus Clouds Above Western Siberia

V. V. Zuev, M. I. Andreev, V. D. Burlakov, A. V. El'nikov, and A. N. Nevzorov
*Institute of Atmospheric Optics
Tomsk, Russia*

Introduction

Cirrus clouds occupy a special place among the earth's cloud formations. Their impact can be manifested through atmospheric warming or cooling (Cox 1971). Recurrence of cirrus clouds and their morphological and microphysical structures undergo significant variations as functions of latitude, season, and orography. Tomsk (56.5°N, 85.1°E) is situated in Western Siberia – a large part of the Eurasian continent covered by large forest areas far from seas and oceans. This introduces specific features in the formation of cirrus cloudiness above Western Siberia. Visual observations and lidar studies of cirrus cloudiness were started in Tomsk in 1997 as part of the Atmospheric Radiation Measurement (ARM) Program. In 1997, the ARM Project envisaged the development of lidar technology and methods for lidar measurements of the characteristics of cirrus clouds as well as the start of observations.

Instrumentation and Experimental Procedure

A lidar system operating at the Siberian Lidar Station is capable of measuring the characteristics of cirrus cloudiness at night and in the daytime. A Nd-YAG laser is used as a transmitter. It generates laser pulses at the wavelength $\lambda=1064$ nm with energy 150 mJ per pulse. The pulse repetition frequency is 10 Hz.

The choice of $\lambda=1064$ nm was determined by the low level of the background daytime sky radiation at this wavelength, which is important for lidar observations of clouds in the daytime. A coaxial transceiver scheme is used in the lidar system. The backscattered laser radiation is received by a mirror with a diameter of 2.2 m and a focal distance of 10 m. A field stop, a collimating lens, a film polaroid, an interference filter, and a focusing lens are placed in the focal plane of the receiving mirror in front of a photomultiplier.

The signal-to-noise ratio was adjusted for daytime and night measurements by changing the diameter of the field stop

and the area of the receiving mirror. In so doing, the entire area of the mirror was used for measurements at night; whereas for daytime measurements the receiving area of the mirror was decreased to that of the mirror 0.3 m in diameter. The field of view of the receiving system was 0.3 mrad. This small field of view was chosen to reduce the background illumination and the contribution of multiple scattering to a lidar return signal. The FEU-83 photomultiplier was used as a receiver. It was cooled by the Peltier elements to a temperature of -30° C to reduce its intrinsic noise level. Lidar return signals were recorded in the photon counting regime. Spatial resolution of the lidar system was 100 m and its temporal resolution was 3 s to 4 s. The lidar system was equipped with a video camera. It was mounted parallel to the lidar optical axis near the focus of the lidar receiving telescope for monitoring the sky cloudiness during lidar measurements. Video records were used to estimate the horizontal cloud sizes as well as the speed and direction of cloud motion.

We measured the characteristics of cloudiness every day from August 8 to September 7, 1997. In so doing, we determined visually the cloud type and the cloud amount every hour from 8:00 a.m. until 8:00 p.m., Tomsk local time. We recorded clouds not only in the zenith, but also in the periphery of the sky. The lidar was oriented in the zenith and measurements were carried out only when clouds fell within the lidar field of view. Time series of lidar return signals were obtained. Each series lasted ~ 30 min and comprised more than 256 individual vertical signal profiles. Every lidar return signal profile was averaged over 20 to 30 laser shots during 3 s to 4 s. Figure 1 shows an example of cloud sensing above the measurement site during half an hour. Cirrus clouds were recorded in the absence of low cloudiness and through it.

To estimate qualitatively the phase state of clouds, in several experiments, we measured the depolarization ratio of lidar return signals. Visual and lidar observations of cirrus cloudiness were carried out in fall and winter. They are being continued now. In this paper, we give only some preliminary results.

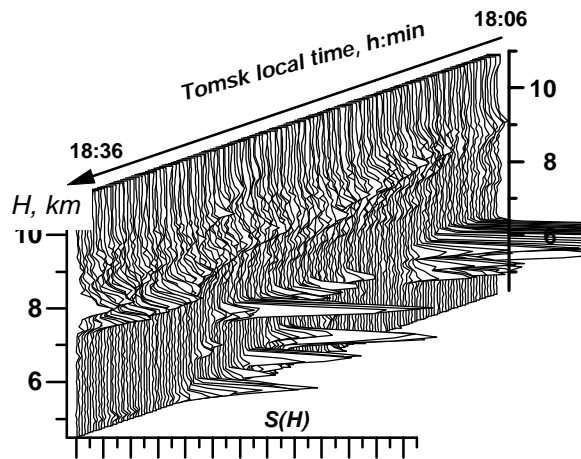


Figure 1. Variations of the vertical structure of lidar return signals corrected for the sensing range during observations of cirrus, high-cumulus, and cumulus cloudiness on August 14, 1997, from 18:06 until 18:36, Tomsk local time.

Some Measurements of Optical and Geometric Characteristics of Cirrus Cloudiness

Small field of view of the lidar receiving system (0.3 mrad) significantly decreased the relative contribution of multiple scattering to a lidar return signal. For this reason, the optical characteristics of clouds were reconstructed in the single scattering approximation. In this case, the backscattering coefficient $\beta_{\pi}(H)$ can be calculated with the use of the well-known procedure for lidar return signal calibration against molecular scattering (Cox 1971) assuming the absence of the aerosol at a given segment of the sensing path. The extinction coefficient $\alpha(H)$ was calculated by the method described in (El'nikov 1991). Under assumption of the constant ratio of the total backscattering coefficient to the total extinction coefficient, the formula for $\alpha(H)$ can be written as

$$\alpha(H) = S(H) \cdot \left[\frac{S(H_c)}{\alpha(H_c)} + 2 \cdot \int_H^{H_c} S(H') dH' \right]^{-1},$$

where H is the altitude, H_c is the calibration altitude, $\alpha(H_c)$ is the value of the extinction coefficient at the calibration altitude (it is considered to be known), $S(H) = [N(H) - N_{bg}] \cdot H^2$ is the lidar return signal $N(H)$ corrected for the sensing range, and N_{bg} is the background sky radiation.

An example of the reconstructed vertical profile of the extinction coefficient on December 22, 1997, is shown in Figure 2 (at the center). This profile was averaged over 256 individual vertical profiles of lidar return signals accumulated from 19:13 till 19:40, Tomsk local time. This allowed us to follow the temporal variability of some parameters of the observed two-layer cloudiness. The heights of the lower (L) and upper (U) cloud boundaries calculated by the criteria of a) 10-fold excess of the backscattering coefficient at the boundary clear atmosphere-cloud (dots) and b) cloud halfwidth (circles) are also shown in Figure 2.

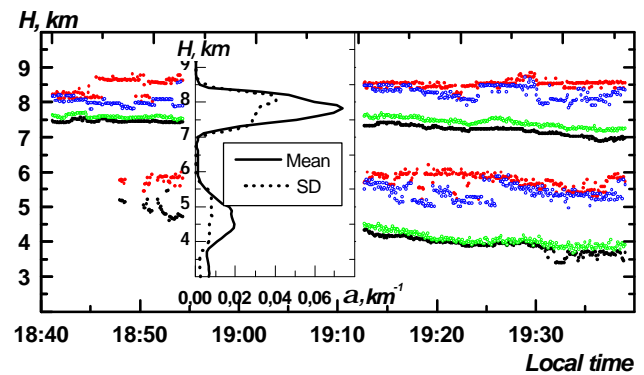


Figure 2. Temporal behavior of the heights of the upper and lower boundaries of the two-layer cloudiness (calculated by the criteria mentioned in the text). The vertical profile of the extinction coefficient averaged over the period from 19:10 until 19:40 and its standard deviation (SD) are shown at the center of the figure. For a color version of this figure, please see http://www.arm.gov/docs/documents/technical/conf_9803/zuev-98.pdf.

Temporal variations of the optical thickness

$$\tau(t) = \int_L^U \alpha(t) \cdot dH$$

of the upper and lower clouds are

illustrated by Figure 3a. Histograms of the distribution of their optical thickness are shown in Figures 3b and 3c. It can be seen that the distribution of the optical thickness of the upper cloud is closer to the normal distribution compared to the lower cloud. The distribution of the optical thickness of the lower cloud is bimodal in character. Its main mode is centered at $\tau=0.04$. The second mode of the distribution centered at $\tau=0.055$ is less pronounced. It is likely that this mode is caused by a wave process, because the Fourier transform has the clearly pronounced maximum near 10^{-2} Hz (Figure 3d).

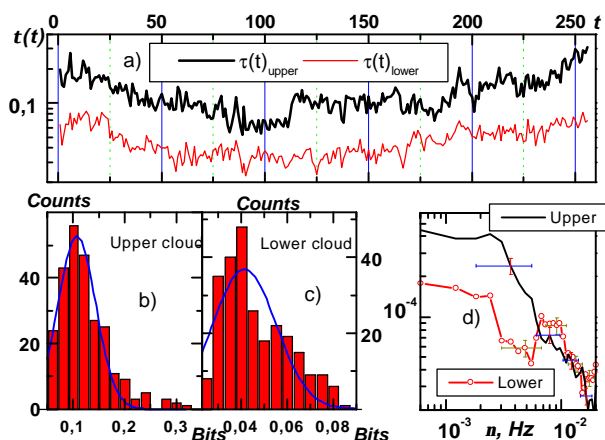


Figure 3. a) Temporal variations of the optical thickness of the upper and lower clouds illustrated by Figure 2 from 19:10 until 19:40, b) and c) histograms of distribution of their optical thickness, and d) their Fourier transforms. For a color version of this figure, please see http://www.arm.gov/docs/documents/technical/conf_9803/zuev-98.pdf.

The vertical profile of the depolarization ratios of lidar return signals $\delta(H)$ ($\delta(H) = P_{\perp}(H) / P_{\parallel}(H)$, where $P_{\perp}(H)$ and $P_{\parallel}(H)$ are the cross-polarized and parallel components of lidar return signals, respectively) within the cloud extended from 6 km to 10.5 km is shown in Figure 4. The cloudiness can be classified as high cumulus by its lower boundary and as cirrus by its upper boundary.

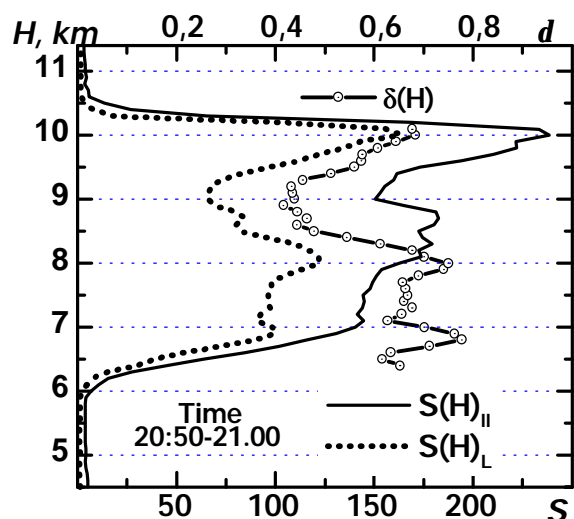


Figure 4. The vertical profiles of the depolarization ratio and parallel and cross-polarized components of the lidar return signal are shown on December 8, 1997.

However, we did not observe any altitude dependence of the statistical or correlation characteristics of cloudiness. Figure 5 shows the temporal autocorrelation functions $K_t(i)$ and the interlevel spatial correlation functions $K_H(i)$ for cloudiness illustrated by Figure 4. The vertical correlation radius ρ_H determined from the halfwidth of these correlation functions is shown in Figure 5. We failed to estimate the correlation time, because already, for the first lag, the slope of the functions $K_t(i)$ exceeded 0.5. However, the first values of the temporal autocorrelation functions $K_t(1)$ that can be used to estimate the correlation time as a function of altitude are shown in Figure 5. At the cloud bottom, the correlation between the levels sharply decreased to near zero in the directions from the cloud boundary toward the cloud depth and toward the clear atmosphere ($K_{6.8 \text{ km}}$). However, at the cloud top (near 9.5 km), the correlation function has the clearly pronounced maximum (~ 0.6). Analogous behavior has $K_{9.6 \text{ km}}$ at the cloud top. The internal cloud layers are closely correlated with the correlation coefficient > 0.7 in the cloud depth ($K_{7.6 \text{ km}}$ and $K_{8.8 \text{ km}}$ in Figure 5). The correlation sharply decreases at the cloud boundaries.

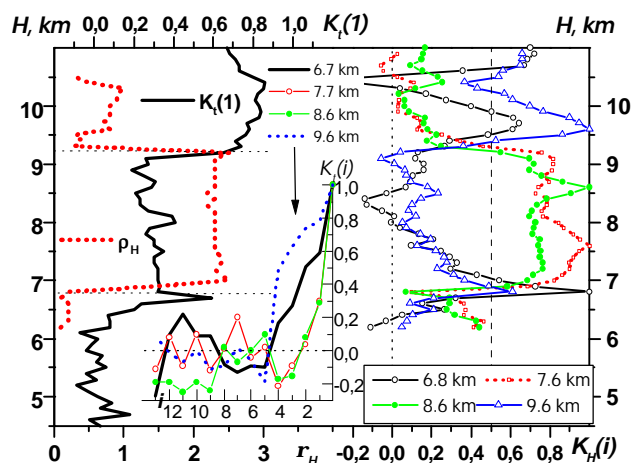


Figure 5. Correlation characteristics of cloudiness displayed in Figure 4 (from 20:15 until 20:35, Tomsk local time). For a color version of this figure, please see http://www.arm.gov/docs/documents/technical/conf_9803/zuev-98.pdf.

Conclusion

Lidar studies of cirrus clouds were started at the Siberian Lidar Station in 1997. A sharp difference between the interlevel correlation functions inside the cloud and at its boundaries (the decreased down to 0.5) was used as a criterion for the determination of the lower and upper cloud boundaries. The recurrence of clouds of all types

(Ci+Cs+Cc) between 6 km and 11 km was 55% over the observation period from August 8 until September 7, which slightly exceeded the reference data (Hahn et al.). The recurrence of Ci was 48%; Cs, 29%; and Cc, 13%. According to the above-mentioned criterion, the recurrence of the cloud base height reached maximum between 7 km and 10 km. Above 11 km, we did not observe the cloud base. Clouds moved preferably to the east with most probable velocities 10 m/s to 20 m/s (in 70% of all cases). In 20% of all cases, the cloud velocities exceeded 20 m/s, and in 10% of all cases, they were less than 10 m/s.

Acknowledgments

We acknowledge with pleasure helpful discussions with Dr. S. V. Smirnov.

References

- Cox S. K., 1971: Cirrus clouds and the climate. *J. Atmos.Sci.*, **28**, 1513-1515.
- El'nikov A. V., Zuev V. V., and Marichev V. N., 1991: *Atmos. Optics*, **4**(2), 201-209.
- Hahn C. J., Warren S. G., London J., Cherwin R. M., and Jenne R. Atlas of simultaneous occurrences of different cloud types over land. - *NCAR Techn.*, Note TN241-STR, 21 p.+188 maps.